Storage of wafer cookies: Assessment by destructive techniques, and non-destructive spectral detection methods

Storage of wafer cookies: assessment by destructive, spectroscopic, and hyperspectral methods

Chiara Cevoli[a], Andrea Evangelisti[a], Paolo Gradari[b], Angelo Fabbri[a]

[a]*Department of Agricultural and Food Sciences, University of Bologna, P.zza Goidanich 60, 47521, Cesena, (FC), Italy*

[b]*Babbi GROUP SpA., Via Caduti di via Fani 80 - 47032 Bertinoro (FC) Italy*

Abstract

Wafer cookies combine two or more layers of wafer sheets with intermediate layers of cream filling and later coating with chocolate. During storage, wafer cookie quality, especially in terms of mechanical properties, is mainly affected by moisture migration from the cream or chocolate and moisture absorption from air. This study aimed to assess the storage of wafer cookies by destructive (water activity, mechanical properties, and sensory acceptance) and non-destructive methods (image analysis, NIR spectroscopy and hyperspectral imaging HSI). Furthermore, two packaging types were considered. Samples were stored at 18°C (RH=50%) and analysed after 2, 4, 5, 6, 7 and 8 months. Good linear relations (R^2 up to 0.84) were found between water activity and mechanical parameters, confirming the dependence between textural aspects and water content. By adding a multi-material packaging layer, the shelf life significantly increased in terms of sensory acceptance (crispness). No significant differences were found between the surface colour parameter (white index) attributable to fat bloom formation. PCA results of NIR and HSI spectra showed a clear separation between samples acquired at time 0 and those analysed during storage that was related with the packaging type and storage time. PLS models developed to estimate the storage time showed R^2 ranging from 0.926 (RMSECV=0.63 months) to 0.960 (RMSECV=0.52 months), while the water activity ranged from 0.858 to 0.928 (RMSECV=0.02). The PLS models based on HSI spectra were used to obtain predictive images of water activity or storage time.

Keywords: wafer, hyperspectral imaging, NIR, storage, packaging.

1. Introduction

Wafer cookies are the result of combining two or more layers of low sugar wafer sheets with intermediate layers of cream filling and later coating with chocolate (Dogan, 2006; Tiefenbacher, 2017). Between packaging and consumption, and thus during storage, the quality of wafer cookies is mainly affected by absorption or moisture shifting. Two potential main sources of moisture absorbed by the wafer can be identified: moisture migration from cream filling or enrobing and moisture sorption from humid air. In the first case, the wafer sheet conditioning (maturing) until reaching the cream and enrobing water activities can significantly reduce the migration. Instead, moisture migration from air during storage is observed when the moisture barrier of the packaging film is not sufficient or sealing of packages is defective (Tiefenbacher, 2017). Wafer moisture modification can directly compromise the product's textural parameters. The texture at first bite and how it breaks up and dissolves in the mouth are the main characteristics, and the crispness is considered a fundamental textural attribute to consider during storage. Water activities of 0.45 and 0.59 are suggested as a significant threshold to lose the wafer's characteristic texture properties (Martinez-Navarrete et al., 2004; Tiefenbacher, 2017). Other food quality parameters, such as oxidation and rancidity, are less significant due to the progress in quality of ingredients and in packaging (Tiefenbacher, 2017). For wafer cookies coated with chocolate, it is important to consider surface colour changes due to the presence of fat bloom. Fat bloom is considered a chocolate defect and is generally characterized by the formation of a dull-white film on the chocolate's surface, negatively impacting quality (Gatti et al., 2021). The exact causes of blooming are still unknown, but improper tempering conditions and temperature fluctuations during storage can promote fat migration through the chocolate's particle matrix with subsequent recrystallization on the surface (Aguilera and Briones, 2005) .

Normally, water activity and textural parameters are determined by destructive methods. (Mohammed et al., 2014, 2013) using uni-axial compression and three-point bending experiments on confectionery wafers to characterise their material behaviour. Concerning wafer sheets, relations between mechanical parameters obtained by a three-point bend test (Force and the distance at the fracture point) and water activity were investigated by (Martinez-Navarrete et al., 2004). Recently, (Nasabi et al., 2021) evaluated the structural properties of wafer sheets made with various sources of grains using a three-point bending probe. Based on our knowledge, no studies on the mechanical parameters of wafers during storage have been carried out.

Considering non-destructive methods, several studies have reported successful application of near infrared (NIR) spectroscopy for moisture and textural determination of intact bakery products as well as their evolution during storage (Cevoli et al., 2015; Chakravartula et al., 2019; Sørensen, 2009; Xie et al., 2003). Furthermore, NIR spectroscopy was applied to quick identification of fat bloom in chocolates after storage at inadequate temperatures of transportation and storage (Gatti et al., 2021).

Hyperspectral imaging (HSI) is a technique that integrates spectroscopy and digital imaging to simultaneously obtain a spectral and spatial three-dimensional data set (hypercube). Recently, HSI has been applied to study the quality and safety attributes of food products as affected by processing and storage (Andresen et al., 2013; Liu et al., 2015). Concerning storage of bakery products, (Sricharoonratana et al., 2021) used the NIR-HSI (935-1720 nm) as a non-destructive method to determine the storage time of freshly baked cakes packed in a polystyrene plastic box. The predictive images showed different colours based on their storage time (0-9 days) that was predicted by a partial least square (PLS) model (R=0.835, RMSECV=1.242 day). (Lancelot et al., 2020) investigated the possibility of using NIR-HSI (950-2500 nm) to quantify the moisture content in two different commercial biscuits stored at different levels of water content (from 0.114 to 0.907). Multi-linear regression (MLR) was used to estimate the moisture content (2.54-23.18 %), reporting an R^2 higher than 0.92. Using the MLR model, false colour images were proposed according to the water content. (Whitworth et al., 2010) presented a spatial evaluation of the moisture distribution for baguette slices

(internal crumb) stored for 96 hours, obtained by applying a calibration modified PLS model to hyperspectral images (950-2495 nm).

Research on the application of HSI on chocolate or cocoa-based products is scarce and no studies have assessed storage. Some studies have examined the authentication and the prediction of fermentation quality parameters of cocoa beans (Caporaso et al., 2018; Cruz-tirado et al., 2020). Only one investigation on chocolate has been carried out and used HSI (4000 to 675 cm^{-1}) combined with multivariate curve resolution to analysis of the constituents of commercial chocolate samples (Zhang et al., 2015).

The aim of the present analysis was to study the storage of wafer cookies coated with chocolate using both destructive (wafer sheet water activity, mechanical properties, and sensory crispness acceptance) and non-destructive methods (image analysis, NIR spectroscopy and Vis/NIR-HSI). Furthermore, two different types of packaging were considered.

2. Materials and Methods

2.1 Samples

The samples examined were vanilla cream-filled wafers (three layers) covered by a thin layer of dark chocolate of about 0.6 mm. The products were supplied by Babbi GROUP SpA. Italy immediately after production. The ingredients of all components (wafer sheet, cream, and chocolate) are reported in Table 1. Half of the samples (n=144) were packaged using the standard packaging (S) adopted by the company, while the other half (n=144) were vacuum-packed (V) adding a multi-material packaging layer (PET and aluminium). The list of the packaging materials is reported in Table 2. Subsequently, samples were stored at 18°C and relative humidity of 50 % for 8 months. Twenty-four samples for each packaging type were collected and analysed after 2, 4, 5, 6, 7 and 8 months of storage. Twelve of these for each storage time were subjected to destructive analysis, while the remaining 12 to non-destructive analysis.

2.2 Destructive analysis

2.2.1 Mechanical properties

A three-point bending test was used to evaluate the mechanical properties of samples according to (Tiefenbacher, 2017) that suggested this test for cream-filled sugar wafer cookies. Measurements were made on 12 samples for each storage time and packaging using a texture analyser (Zwick Roell 500N) equipped with a load cell of 100 N. The sample was placed on two holders fixed at 35 mm distance, while a parallelepiped (6x6x50 mm) was used as probe. The probe moved down for 20 mm at a speed of 1.5 mm/s.

2.2.2 Water activity

The water activity (Aqualab Pawkit, water activity meter, Decagon Devices) was measured on the internal wafer sheets collected from each sample (12 samples for each storage time and packaging type). Before proceeding with the analysis, the cream and chocolate were removed.

2.2.3 Sensory test

The trained panel was composed of six people employed by the collaborating company. Each panellist evaluated texture at first bite assigning a score between 1 and 10 based on the crispness (a combination of the type of sound (i.e., short snapping and longer cracking sounds) and the force to bite and chew as perceived on first bite (Duizer and Winger, 2006)). According to the criteria adopted by the company, the acceptable limit of crispness was 6 (1 = not crisp - totally not acceptable, 10 = very crisp -totally acceptable).

2.2.4 Data analysis

Significant differences between means of the destructive parameters at different storage times, within the same packaging type, were explored using ANOVA (post doc: Tukey's HSD, p-level < 0.05). Subsequently, possible statistical relations between parameters were investigated (Matlab2018a®).

2.3 Non-destructive analysis

2.3.1 Image analysis

Colour surface evaluation was carried out using an electronic eye (visual analyser VA400 IRIS Alpha M.O.S., France) composed of a chamber (420 x 560 mm), LED light system [98 CRI (colour rendering index), D65 (light of a cloudy day at 12:00), 6700 °K (colour temperature)] and a CCD camera (16 million colours). Light and camera were in the upper part of the system. The built-in zoom was automatically calibrated by the software (E-Eye software Alpha-Soft, version 14.0). The analysis was set up with a resolution of 1214×911 pixels. Images were acquired by placing samples at 80 mm from the camera. Raw images were processed in RGB scale and subsequently converted in Cie$L^*a^*b^*$ scale. For each wafer image, the white background was automatically removed and the mean L^*, a^* and b^* values were calculated considering the wafer region. Subsequently, the white index (WI) was calculated, as reported by (Kumara et al., 2003; Popov-Raljić and Laličić-Petronijević, 2009):

$$\mathrm{WI} = 100 - \left[(100 - L^*)^2 + a^{*2} + b^{*2}\right]^{1/2}$$

2.3.2 NIR spectroscopy

Samples were evaluated with an FT-NIR spectrophotometer (MATRIX ™ –F, Bruker Optics) in diffuse reflectance in the range from 833 to 2500 nm (8 cm^{-1} resolution). Three scans were obtained by placing the optical fibre probe (IN 261, Bruker Optics, Mass., USA) in direct contact with the product surface at three different points. The background was acquired by placing the probe in a support covered made of spectralone and subsequently subtracted from each spectrum. The mean spectrum of the three acquisitions was calculated and used for chemometric elaboration.

The first part of the spectra until 1000 nm was deleted as it contains no useful chemical information, but only instrumental noise. Subsequently, absorbance data were normalised using the Standard Normal Variate (SNV) technique. To remove both additive and multiplicative effects, spectra were treated by applying the first Savitzky–Golay derivative (D1) and then mean cantered (MC). PCA

analysis was used as an explorative technique to group samples as a function of packaging type and storage time. Subsequently, PLS models were developed to estimate the storage time and water activity considering the samples together and split by type of packaging. The models were validated by the venetian blind cross-validation method (segments: 10), while the permutation test was used to evaluate the model robustness and significance. To avoid the model over-fitting, the optimal number of latent variables (LV) were chosen by detecting the global minimum of root mean square error in cross validation (RMSECV).

The data elaboration was carried out by using PLS Toolbox for Matlab2018a®.

2.3.3 Hyperspectral imaging

A push-broom linear array hyperspectral camera working from 400 to 1000 nm for a total of 272 bands (Nano-Hyperspec VNIR, Headwall Photonics, Inc., Fitchburg, MA, USA) and characterised by a spatial resolution of 640 points was adopted to acquire HS images. The camera was equipped with a focal lens of 17 mm, and was installed with the optical axis perpendicular to the underlying conveyor belt (speed of 8 mm/s) at a height of 540 mm. Two halogen lamps (120 W), inclined by 15 °, were installed at about 320 mm from the conveyor belt plane. Ambient light was isolated using a specific box. The sensor exposure time and frame period were set at 30 ms. The white and dark reference reflectance spectra were obtained by acquiring a high-reflectance matte white panel (R_w) and covering the camera lens with its cup (R_d), respectively. Each sample was scanned longitudinally to obtain the raw reflectance spectrum (R_r). The calibrated reflectance (R_c) was subsequently calculated:

$$R_c = \frac{R_r - R_d}{R_w - R_d}$$

The region of interest (ROI) was selected by the k-means clustering method (Euclidean distance), performed using 3 clusters (figure 1) [cluster 1: background to be discarded (light grey); cluster 2:

sample shadow (dark grey); cluster 3: ROI (black)]. For each sample, the ROI mean spectrum was calculated and converted from reflectance to absorbance.

Spectral bands between 400 and 450 nm were removed due to a low signal-to-noise ratio produced by the sensor.

The spectra were smoothed (Savitzky-Golay method; polynomial order: 2; smoothing points: 15) to reduce noise from the spectra (Amigo et al., 2013), and subsequently pre-processed by SNV, D1 and MC. AS for NIR spectroscopy, PCA analysis was used as an explorative technique to group samples as a function of packaging type and storage times, and the PLS models to estimate the storage time and water activity considering together the samples and split by type of packaging. Predictive models were validated by the venetian blind cross-validation method (segments: 10), and to avoid the model over-fitting, the optimal number of latent variables (LV) were chosen by detecting the global minimum of root mean square error in cross validation (RMSECV). Permutation test was used to evaluate the model robustness and significance. Finally, PLS models were used to obtain predictive spectral maps of water activity or storage time distribution. Results of the estimated value from the models were interpolated in each pixel of the hyperspectral image.

The data elaboration was carried out by using PLS Toolbox and MIA Toolbox for Matlab2018a®.

3. Results

The mean and standard deviation of the water activity of the wafer sheet measured during the storage are reported in Table 3, for both the packaging type (standard: S, vacuum: V). A significant increase was observed from 0 to 2 months of storage (passing from 0.27 to 0.38) after which the mean values remained constant until 5 (S) and 6 (V) months. Finally, the water activity increased reaching values of 0.47 (S) and 0.42 (V) after 8 months of storage. For the same storage time, significant differences between the mean values of the two types of packaging were achieved starting from 6 months. To avoid moisture migration from the cream during storage, the wafer sheets were conditioned until reaching a water activity value near to that of the cream (0.26). Consequently, the increase in water

activity is probably due to ambient humidity. The primary packaging was not sealed, and consequently the first Aw increases (from 0.27 to 0.38), found for both packaging types, was likely due to the humidity present in the headspace of the second packaging.

From force-distance curves, the force (Fmax) and distance (D) at the first yield points were identified and reported in Table 3 as a function of storage time and packaging type. An initial increase in both mechanical parameters was observed passing from 0 to 2 months. These trends can be attributed to the significant Aw increase (from 0.28 to 0.38), and reflect in an increase in sample deformability, which in turn increases its resistance to fracture. For both packaging types, from 2 to 6 months, no significant differences were observed between the means, with limited variations in water activity (from 0.38 to 0.40). After 6 months, the D parameter increased reflecting the progressive plasticising effect of water in the product, becoming more deformable in line with the increase in water mobility associated with water interaction (Martinez-Navarrete et al., 2004). Good linear relations (S: R^2=0.84; V: R^2=0.78) were found between water activity and mean values of D, confirming the dependence of mechanical behaviour on the effect of the water on the water sheet (Tiefenbacher, 2017).

evaluated texture at first bite assigning a score between 1 and 10 based on the crispness (a combination of the type of sound (i.e., short snapping and longer cracking sounds) and the force to bite and chew as perceived on first bite (Duizer and Winger, 2006)). According to the criteria adopted by the company, the

Sensory acceptance related to product crispness, was evaluated by six trained panellists. The scale ranged from 1 (not crisp - totally not acceptable) to 10 (very crisp -totally acceptable) and the acceptable limit of crispness was 6. At lower values, the product is commercially unacceptable. The mean values, as a function of storage time and packaging type, are shown in Figure 2a. Sensory acceptance related to crispness linearly decreased with storage time, which was more pronounced for samples stored in standard packaging (S=-0.6347; V=-0.2186). Furthermore, the acceptance of samples packaged under vacuum did not reach the unacceptable level (6), while the samples in standard packaging reached this level after 6/7 months. Accordingly, the shelf life of the products

packaged in standard conditions defined by the company is 6 months. Relations between sensory acceptances and water activities (Figure 2b) or mechanical parameters D (Figure 2c) were investigated. In both cases (Aw and D), stronger linear relations were found considering the samples packaged under vacuum (R^2=0.82 and 0.91), probably due to a more accentuated linearity between acceptance and storage time. The acceptance limit (6) corresponds to a wafer sheet water activity of about 0.44. This Aw value is in agreement with those (0.40-0.45) reported by (Tiefenbacher, 2017) regarding the limit to define "good" and "compromised" wafers in terms of sensory (textural) properties.

Chocolate colour changes, mainly related to fat bloom, were evaluated considering the WI as reported by other studies (Kumara et al., 2003; Popov-Raljić and Laličić-Petronijević, 2009). Bloom can appear in either a uniform white film or as spots randomly placed on the chocolate surface. Consequently, mean WI values calculated on the entire top surface of the wafers were considered. Means and standard deviations obtained considering 12 samples for each storage time and packaging type are reported in Table 3. These values are in the same range as those reported in several studies on dark chocolate (Popov-Raljić and Laličić-Petronijević, 2009). No significant differences were found between the mean values with the same packaging time, and between the two different packages for the same storage times. Very restricted variations of mean values were observed, passing from 31.9 to 32.8. This confirms that there was no evident fat bloom formation during storage due to improper temperature or temperature fluctuations during storage.

Figure 4 shows the NIR spectra of all samples from 833 to 2200 nm. The range from 2200 to 2500 nm was removed due to instrumental noise. Two spectral pre-treatments were reported, SNV (Figure 3a) and first derivative (Figure 3b). Considering that the penetration depth of NIR radiation in food is approximately 1 mm (Almeida et al., 2006; Huang et al., 2016), the spectra are mainly affected by the dark chocolate (thickness of 0.6 mm). However, there may also be an influence on the wafer sheet composition. Cocoa butter is the main ingredient in chocolate, although it also contains sugar and cocoa mass. These ingredients contribute to the spectral signals because of the presence of peptide

and covalent bonds, proteins, carbohydrates and lipids (Gatti et al., 2021; Giovenzana et al., 2015; Moros et al., 2007). For all samples, it is possible to identify peaks to around 1730, and 1760 nm which match the C-H bonds in CH_2 groups (cocoa butter). Fatty acids and esters can be associated with absorption bands at 1180, 1215, 2145 and 2190 nm, and amide II and amide III at 2010 and 2050 nm, respectively (small amount of protein). Moreover, spectra show peaks at 1440 nm and 2080 nm corresponding to O-H absorbance in sugar. The small amount of water, mainly present in the wafer sheet, could be identified at around 1930 nm. Consequently, according to the increases in water activity, especially from 0 to 2 months of storage, notable differences were found in the spectral range from 1900 to 2000 nm between the samples analysed at time 0 (black lines) and during storage (grey lines).

PCA analysis was used as an explorative technique to group samples as a function of packaging type and storage time. The score plot obtained considering all samples in the spectral range from 1000 to 2200 nm is shown in Figure 4a. A clear separation between samples acquired at time 0 (black squares) and those analysed during storage (grey symbols) was mainly observed along PC2 (12.25 %). Samples stored in standard (S) and vacuum (V) packaging can be grouped considering the PC1 and PC2. Evaluating the X-loading plot (Figure 4b), it was possible to assert that the discrimination along the PC2 is due to the NIR region from 1850 to 2000 due to the significant increase in water content from 0 to 2 months of storage.

Considering only the samples analysed during storage (from 2 to 8 months), three additional PCA were developed for both (Figure 5a) and single (Figure 5b and 5c) packaging types. The score plots showed notable sample distributions along PC1 according to storage time, passing from 2 to 8 months. This behaviour was more pronounced for samples stored in standard packaging, which is probably due to the greater increase in water activity. Also, in this case the highest X variable variances associated with the highest X-loadings were observed in the range from 1800 to 2000 nm (water band). Changes in the spectral ranges characteristic of fats were not observed, thus confirming that there was no fat bloom formation in chocolates (Gatti et al., 2021) as deduced by the colour analysis.

PLS models were developed to estimate the storage time and water activity from NIR data considering the spectral range from 1000 to 2200 nm. The results, in terms of determination coefficient (R^2) and root mean square error (RMSE), are reported in Table 4. The model's robustness, according to the number of selected latent variables (LVs), was evaluated with a permutation test. *P*-values lower than 0.05 were obtained for cross-validation by employing a randomization t-test, thus confirming the significance of the original models at a 95% confidence level.

. R^2 (cross-validation) from 0.926 (RMSECV=0.63 months) to 0.960 (RMSECV=0.52 months) and from 0.858 (RMSECV=0.02) to 0.924 (RMSECV=0.02) were achieved for storage time and water activity, respectively. In general, the best performances were obtained for storage time and considering separately the samples stored in standard and vacuum packaging.

Figure 6 shows the mean Vis/NIR spectra (calculate considering the ROI of the hyperspectral images) of all samples in the wavelength range from 450 to 1000 nm. Two spectral pre-treatments were reported, namely SNV (Figure 7a) and D1 (Figure 7b). The absorbance spectra are similar to those reported by (Fernandes et al., 2018; Millar and Hall, 2005) for dark chocolate and cocoa samples, respectively. As expected, the highest absorbances were observed in the VIS range, until 700 nm, due to the sample's dark colour. The first derivative allowed to emphasise the presence of peaks and highlight differences between the spectra.

The PCA score plot obtained considering all samples in the spectral range from 450 to 1000 nm is shown in Figure 7a. A clear separation between samples acquired at time 0 (black squares) and those analysed during storage (grey symbols) was observed along PC1 (56.59 %) and PC2 (23.92 %). The X-loading plot (Figure 7b) suggests that the discrimination might be attributed to the Vis absorption region, especially around 500 and 650 nm which is associated with blue and red colours, respectively. These two bands were also proposed by (Fernandes et al., 2018) as absorption maxima of cocoa beans in the Vis/NIR range. Sample discrimination was not observed according to the packaging type and storage time. Subsequently, only the NIR range (700-1000 nm) and samples analysed during the storage (from 2 to 8 months) were considered. The PCA score plot showed sample distributions along

PC2 according to the storage time, passing from 2 to 8 months, for both packaging types (Figure 8). As for the NIR spectroscopy results, the discrimination was more pronounced for samples stored in standard packaging.

As for NIR data, PLS models were developed to estimate the storage time and water activity. Considering the PCA results, only the spectral range from 7000 to 1000 nm was taken into account. The results, in terms of R^2, RMSE and number of LV (model robustness tested by permutation test with $p<0.05$) are reported in Table 4. R^2 (cross-validation) from 0.931 (RMSECV=0.62 months) to 0.956 (RMSECV=0.55 months) and from 0.869 (RMSECV=0.02) to 0.928 (RMSECV=0.02) were obtained for storage time and water activity, respectively. The best performances were obtained for the storage time considering separately the samples stored in standard and vacuum packaging. Very similar PLS results were achieved for both spectroscopic techniques.

The calibration PLS models were used to obtain predictive spectral images based on their water activity or storage time. In particular, the water activity or storage time spatial distribution was achieved by interpolating the results of the estimated value from the models in each pixel of the hyperspectral image. The prediction maps of three representative samples (samples stored in standard packaging) are shown in Figure 9. The colour bar (from blue to yellow) indicates the scale of the reference values (water activity from 0.2 to 0.5; storage time from -1 to 10 months). For both references values, the spatial distributions are in alignment with the measured values. The mean predicted water activity was 0.27 (A), 0.40 (B) and 0.46 (C), while for the storage time was 0.2 (A), 3.9 (B) and 7.6 (C) months. The non-homogeneous colour distribution suggests that there was a spectral variation as a function of the pixel position. This is probably due to the product surface heterogeneity related to the wafer texture, and a possible non-uniform distribution of the chocolate layer, affecting the physical and chemical properties of each pixel (Chen et al., 2021).

Conclusions

The storage of wafer cookies packaged with two different packaging was assessed using destructive (water activity, mechanical properties, and sensory acceptance) and non-destructive methods (image analysis, NIR spectroscopy and hyperspectral imaging). Good linear relations were found between water activity and mechanical parameters, confirming that changes in wafer moisture can directly compromise the product's textural parameters. A correspondence between sensory acceptance limit (6) and the water activity value of 0.44 was found. Other studies defined this water activity value as the limit to describe "good" and "compromised" wafers, in terms of sensory (textural) properties. The packaging characterised by the addition of a multi-material layer significantly affected the product's shelf-life in terms of sensory acceptance. The surface colour (white index) was not changed, confirming there was no evident fat bloom formation during storage due to improper temperature or temperature fluctuations. NIR spectroscopy and hyperspectral imaging allowed to determine the storage time and water activity in real-time and in a non-destructive manner, and to detect differences according to the type of packaging. Furthermore, hyperspectral imaging permitted visualization of the spatial distribution of the water activity and storage time.

References

Aguilera, M., Briones, V., 2005. Image analysis of changes in surface color of chocolate. Food Res. Int. 38, 87–94. https://doi.org/10.1016/j.foodres.2004.09.002

Almeida, M., Torrance, K.E., Datta, A.K., Almeida, M., 2006. Measurement of Optical Properties of Foods in Near- and Mid-Infrared Radiation. Int. J. Food Prop. 29, 651–664. https://doi.org/10.1080/10942910600853667

Amigo, J.M., Marti, I., Gowen, A., 2013. Hyperspectral Imaging and Chemometrics : A Perfect Combination for the Analysis of Food Structure , Composition and Quality, in: Marini, F. (Ed.), Data Handling in Science and Technology. Elsevier B.V., Amsterdam: The Netherlands, pp. 343–370. https://doi.org/10.1016/B978-0-444-59528-7.00009-0

Andresen, M.S., Dissing, B.S., Hanne, L., 2013. Quality assessment of butter cookies applying

multispectral imaging. Food Sci. Nutr. 1, 315–323. https://doi.org/10.1002/fsn3.46

Caporaso, N., Whitworth, M.B., Fowler, M.S., Fisk, I.D., 2018. Hyperspectral imaging for non-destructive prediction of fermentation index , polyphenol content and antioxidant activity in single cocoa beans. Food Chem. 258, 343–351. https://doi.org/10.1016/j.foodchem.2018.03.039

Cevoli, C., Gianotti, A., Troncoso, R., Fabbri, A., 2015. Quality evaluation by physical tests of a traditional Italian flat bread. Eur. Food Res. Technol. 240, 1081–1089. https://doi.org/10.1007/s00217-015-2429-7

Chakravartula, S.S.., Cevoli, C., Balestra, F., Fabbri, A., Dalla, M., 2019. Evaluation of the effect of edible coating on mini-buns during storage by using NIR spectroscopy. J. Food Eng. 263, 46–52. https://doi.org/10.1016/j.jfoodeng.2019.05.035

Chen, Z., Wang, Q., Zhang, H., Nie, P., 2021. Hyperspectral Imaging (HSI) Technology for the Non-Destructive Freshness Assessment of Pearl Gentian Grouper under Different Storage Conditions. Sensors 21, 1–13. https://doi.org/https://doi.org/10.3390/s21020583

Cruz-tirado, J.P., Antonio, J., Barbin, F., Baeten, V., 2020. Authentication of cocoa (Theobroma cacao) bean hybrids by NIR-hyperspectral imaging and chemometrics. Food Control J. 118, 107445. https://doi.org/10.1016/j.foodcont.2020.107445

Dogan, I.S., 2006. Original article Factors affecting wafer sheet quality. Int. J. Food Sci. Technol. 41, 569–576. https://doi.org/10.1111/j.1365-2621.2005.01117.x

Duizer, L.M., Winger, R.J., 2006. Instrumental measure of bite forces associated with crisp products. J. Texture Stud. 37, 1–15.

Fernandes, D., Leonardo, B., Maciel, F., Henrique, C., Bazoni, V., Ribeiro, S., Duarte, R., Carvalho, S., Bispo, S., Yoko, E., Spı, P., 2018. Classification and compositional characterization of different varieties of cocoa beans by near infrared spectroscopy and multivariate statistical analyses 55, 2457–2466. https://doi.org/10.1007/s13197-018-3163-5

Gatti, R.F., Santana, F.B. De, Poppi, R.J., Ferreira, D.S., 2021. Portable NIR spectrometer for quick identification of fat bloom in chocolates. Food Chem. 342, 128267.

https://doi.org/10.1016/j.foodchem.2020.128267

Giovenzana, V., Beghi, R., Hassinger, A.P.., Guidetti, R., 2015. Assessment of Tempering Degree during the Chocolate Pre-Crystallisation Phase Using near Infrared Spectroscopy. NIR news 26, 8–10. https://doi.org/https://doi.org/10.1255/nirn.1501

Huang, M., Kim, M.S., Chao, K., Qin, J., Mo, C., Esquerre, C., Delwiche, S., Zhu, Q., 2016. Penetration Depth Measurement of Near-Infrared Hyperspectral Imaging Light for Milk Powder. Sensors 16, 1–11. https://doi.org/10.3390/s16040441

Kumara, B., Jinap, S., Man, Y.B.C., Yusoff, M.S.A., 2003. Note : Comparison of Colour Techniques to Measure Chocolate Fat Bloom. Food Sci. techology Int. 9, 295–299. https://doi.org/10.1177/108201303036045

Lancelot, E., Courcoux, P., Chevallier, S., Le-Bail, A., Jaillais, B., 2020. Prediction of water content in biscuits using near infrared hyperspectral imaging spectroscopy and chemometrics. J. Near Infrared Spectrosc. 28, 140–147. https://doi.org/10.1177/0967033520902538

Liu, D., Zeng, X.A., Sun, D.W., 2015. Recent Developments and Applications of Hyperspectral Imaging for Quality Evaluation of Agricultural Products: A Review. Crit. Rev. Food Sci. Nutr. 55, 1744–1757. https://doi.org/10.1080/10408398.2013.777020

Martinez-Navarrete, N., Moraga, G., Talens, P., Chiralt, A., 2004. Water sorption and the plasticization effect in wafers. Int. J. Food Sci. Technol. 39, 555–562. https://doi.org/10.1111/j.1365-2621.2004.00815.x

Millar, S., Hall, A., 2005. Evaluating chocolate blends [WWW Document]. NEW Food. URL https://www.newfoodmagazine.com/article/2320/evaluating-chocolate-blends/

Mohammed, I.K., Charalambides, M.N., Williams, J.G., Rasburn, J., 2014. Modelling the microstructural evolution and fracture of a brittle confectionery wafer in compression. Innov. Food Sci. Emerg. Technol. 24, 48–60. https://doi.org/10.1016/j.ifset.2013.11.015

Mohammed, I.K., Charalambides, M.N., Williams, J.G., Rasburn, J., 2013. Modelling the deformation of a confectionery wafer as a non-uniform sandwich structure 2462–2478.

https://doi.org/10.1007/s10853-012-7034-6

Moros, J., Inos, F.., Garrigues, S., Guardia, M. De, 2007. Near-infrared diffuse reflectance spectroscopy and neural networks for measuring nutritional parameters in chocolate samples. Anal. Chim. Acta 584, 215–222. https://doi.org/10.1016/j.aca.2006.11.020

Nasabi, M., Naderi, B., Akbari, M., Aktar, T., Kieliszek, M., 2021. Physical , structural and sensory properties of wafer batter and wafer sheets influenced by various sources of grains. LWT - Food Sci. Technol. 149, 111826. https://doi.org/10.1016/j.lwt.2021.111826

Popov-Raljić, J. V., Laličić-Petronijević, J.G., 2009. Sensory Properties and Color Measurements of Dietary Chocolates with Different Compositions During Storage for Up to 360 Days. Sensors 9, 1996–2016. https://doi.org/10.3390/s90301996

Sørensen, L.K., 2009. Application of reflectance near infrared spectroscopy for bread analyses. Food Chem. 113, 1318–1322. https://doi.org/10.1016/j.foodchem.2008.08.065

Sricharoonratana, M., Keith, A., Teerachaichayut, S., 2021. Use of near infrared hyperspectral imaging as a nondestructive method of determining and classifying shelf life of cakes. LWT - Food Sci. Technol. 136, 110369. https://doi.org/10.1016/j.lwt.2020.110369

Tiefenbacher, K.F., 2017. The Technology of Wafers and Waffles I Operational Aspects, 1st Editio. ed. Academic Press Elsevier.

Whitworth, M.B., Millar, S.., Chau, A., 2010. Food quality assessment by NIR hyperspectral imaging, in: SPIE Defense, Security, and Sensing, Orlando, Florida (USA). pp. 1–12.

Xie, F., Floyd, E.., Xiuzhi, S.., 2003. Comparison of near-infrared reflectance spectroscopy and texture ... Cereal Chem. 80, 25–29.

Zhang, X., de Juan, A., Tauler, R., 2015. Multivariate Curve Resolution Applied to Hyperspectral Imaging Analysis of Chocolate Samples. Appl. Spectrosc. 69, 993–1003. https://doi.org/10.1366/14-07819

Figure captions

Figure 1. Selection of the region of interest (ROI) by k-means clustering (cluster 1: background; cluster 2: sample shadow; cluster 3: ROI)

Figure 2. Sensory acceptance as a function of storage time (a), water activity (b) and distance (D) mechanical parameter (c). S: standard packaging, V: vacuum packaging.

Figure 3. NIR spectra: a) Standard Normal Variate (SNV) pre-processing; b) first derivative (D1) pre-processing (S: standard packaging, V: vacuum packaging; t0: initial storage time).

Figure 4. Results of the PCA model developed considering all NIR spectra (from 1000 to 2200 nm, SNV+D1+MC pre-processing): a) score plot (PC1 *vs* PC2), b) X-loadings of the first two component. (S: standard packaging, V: vacuum packaging; t0: initial storage time).

Figure 5: Score plots (sample *vs* PC1) of the PCA models developed considering only the NIR spectra (from 1000 to 2200 nm, SNV+D1+MC pre-processing) of samples analysed during storage (from 2 to 8 months): a) samples stored in standard and vacuum packaging; b) samples stored in standard packaging; c) samples stored in vacuum packaging

Figure 6: Vis/NIR HSI spectra: a) Standard Normal Variate (SNV) pre-processing; b) first derivative (D1) pre-processing (S: standard packaging, V: vacuum packaging.).

Figure 7. Results of the PCA models developed considering all Vis/NIR HSI spectra (from 500 to 1000 nm; SNV+D1+MC pre-processing): a) score plot (PC1 *vs* PC2), b) X-loadings of the first two component. (S: standard packaging, V: vacuum packaging; t0: initial storage time).

Figure 8. Score plot (PC2) of the PCA model developed considering only the vis/NIR HSI spectra (from 700 to 1000 nm, SNV+D1+MC pre-processing) of samples analysed during storage (from 2 to 8 months).

Figure 9. Prediction maps of water activity and storage time of three representative wafer cookies stored in standard packaging (A=0 months, B=4 months; C=8 months).

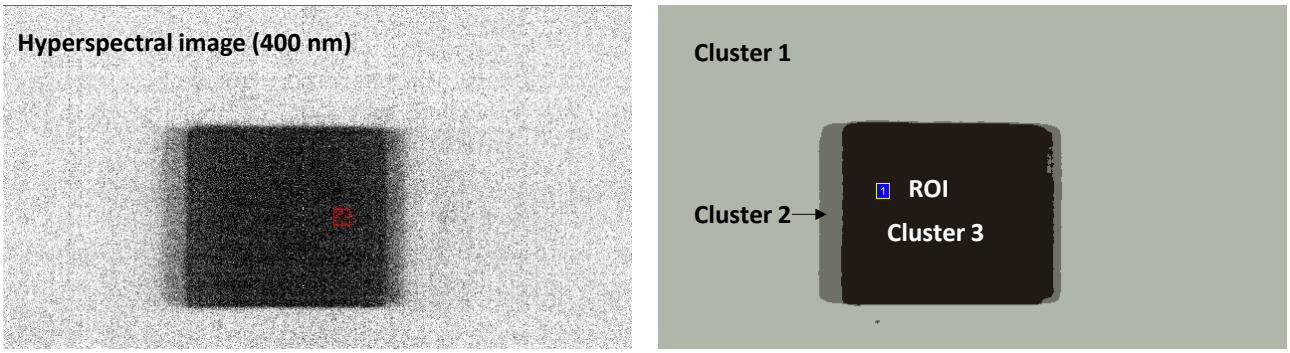

464

465 Fig.1

466

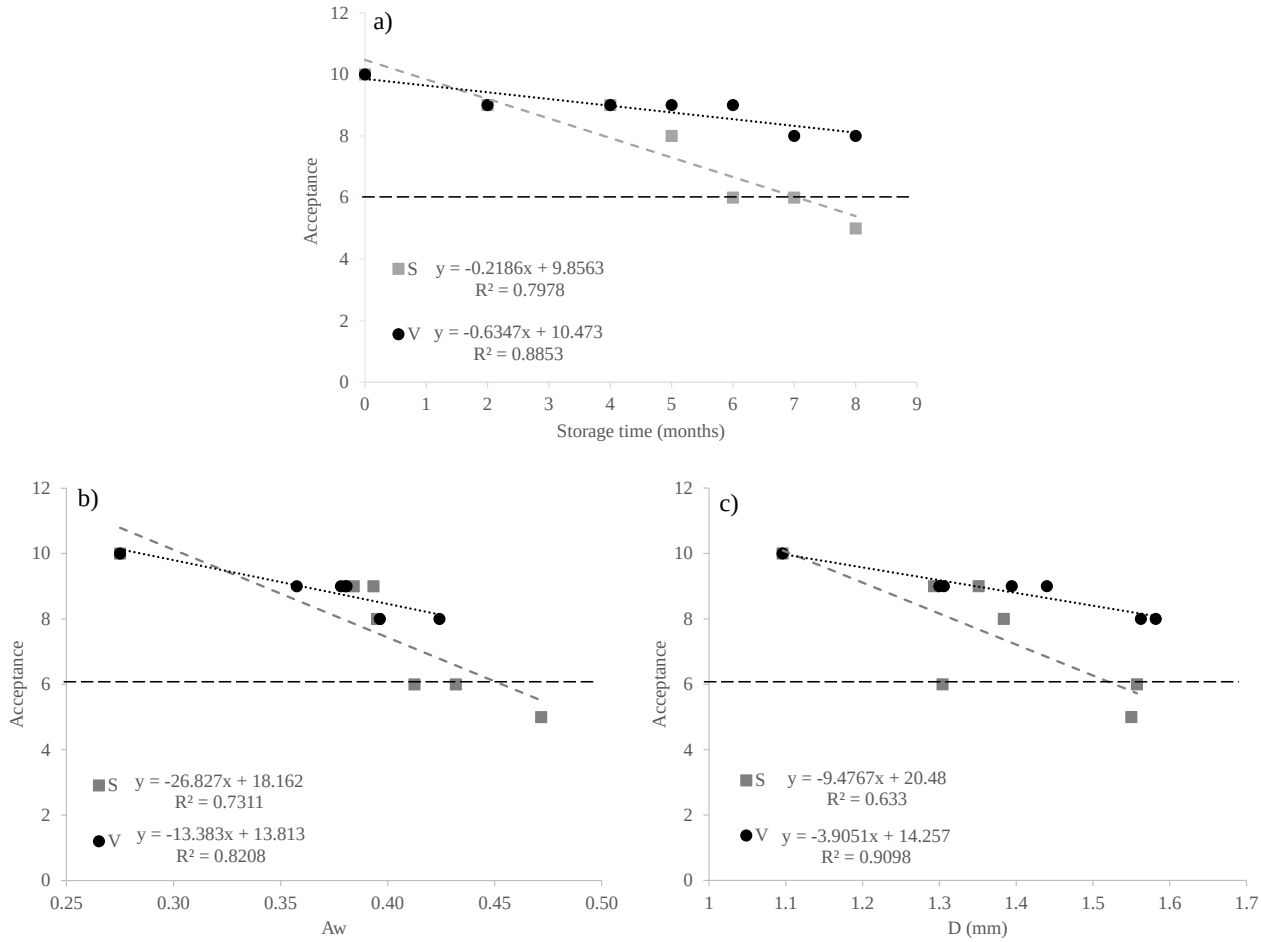

467

468 Fig.2

469

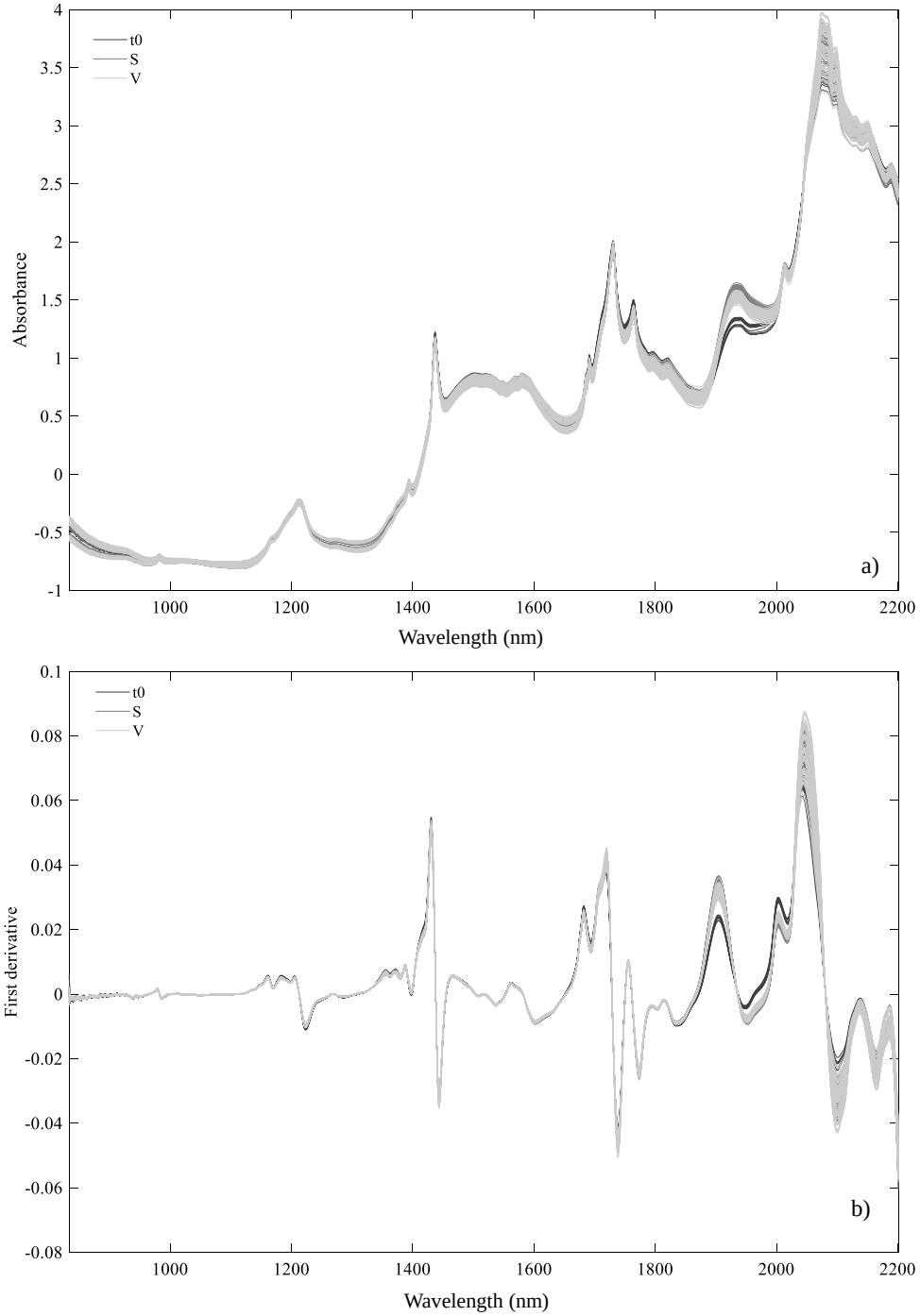
t0
S
V
Absorbance
Wavelength (nm)
a)
First derivative
Wavelength (nm)
b)

Fig.3

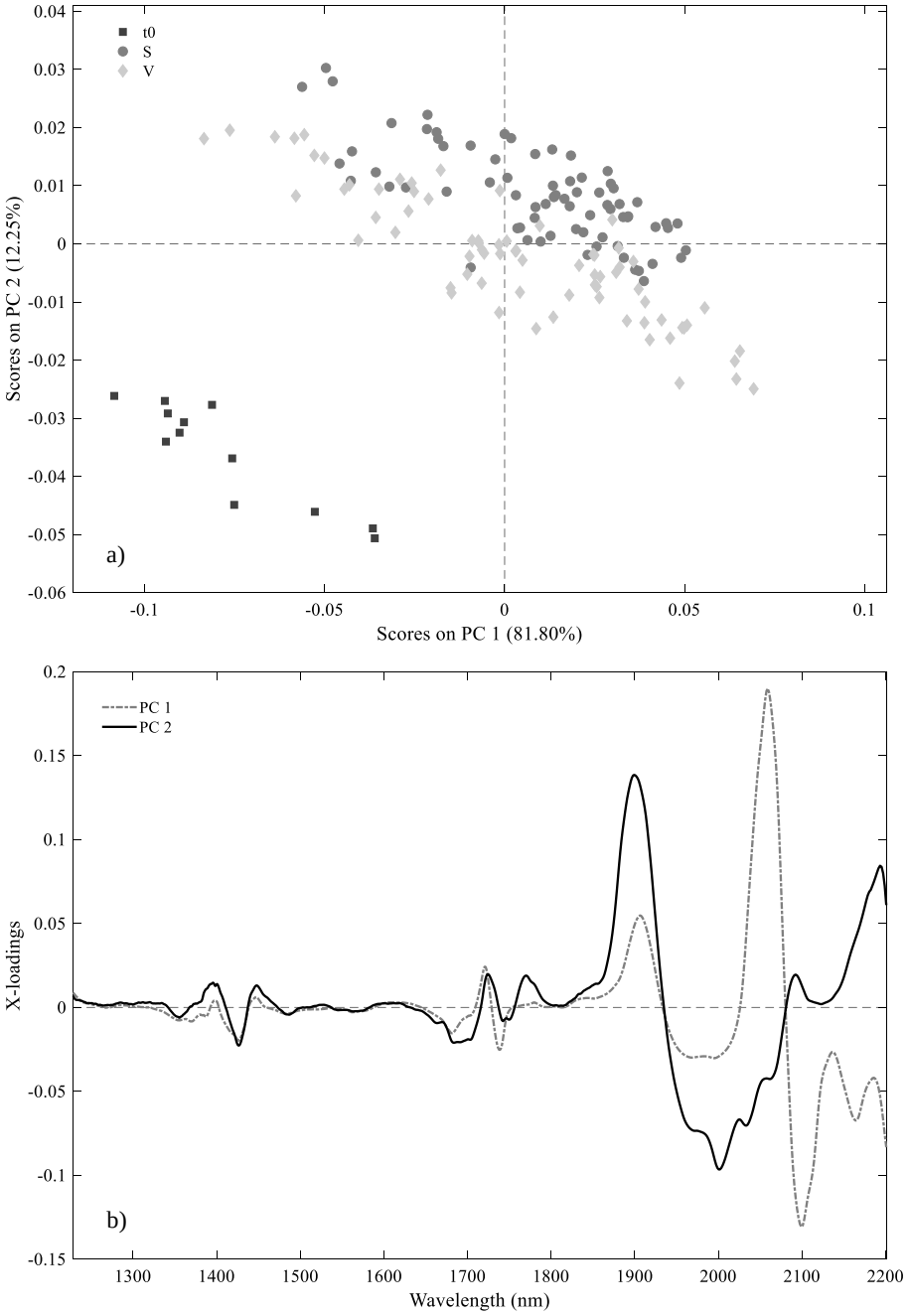

473

474 Fig.4

475

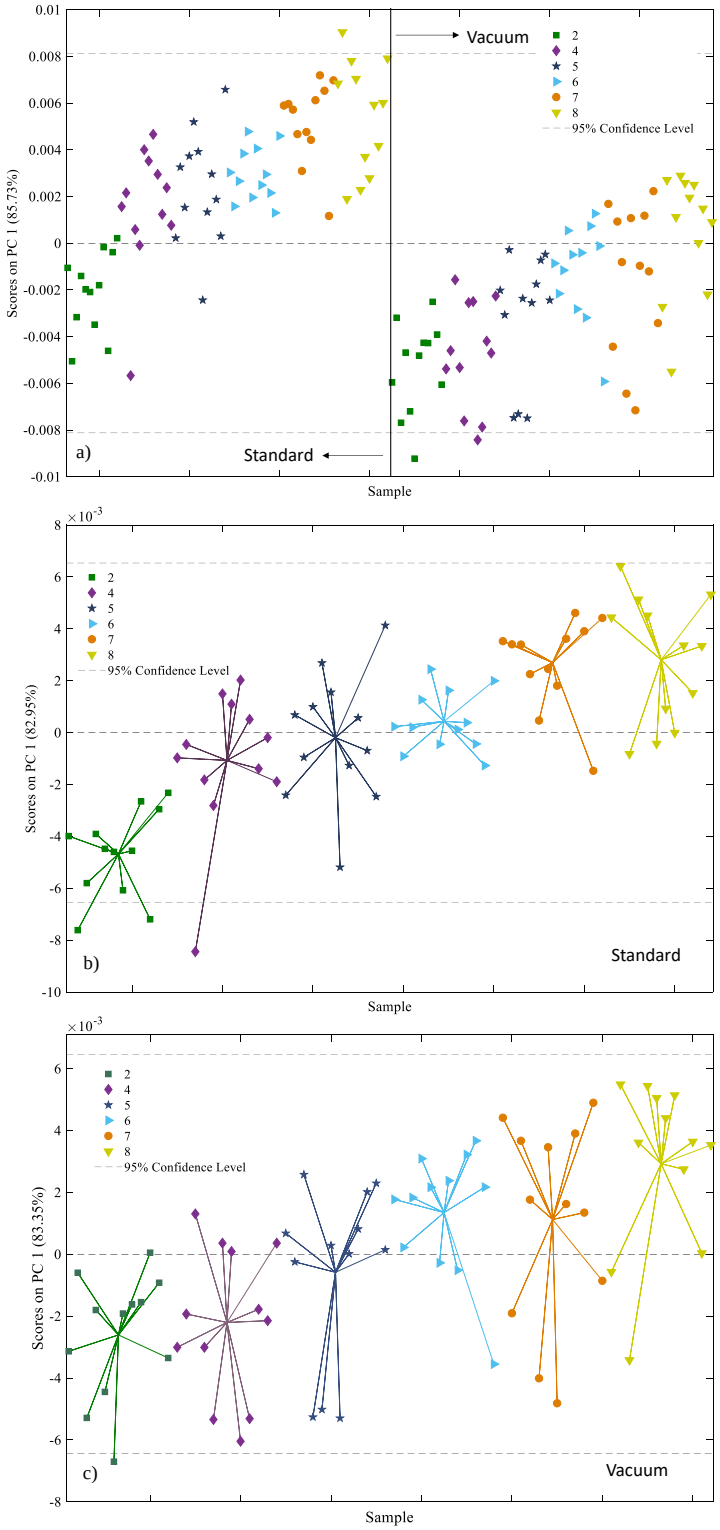

476

477 Fig.5

478

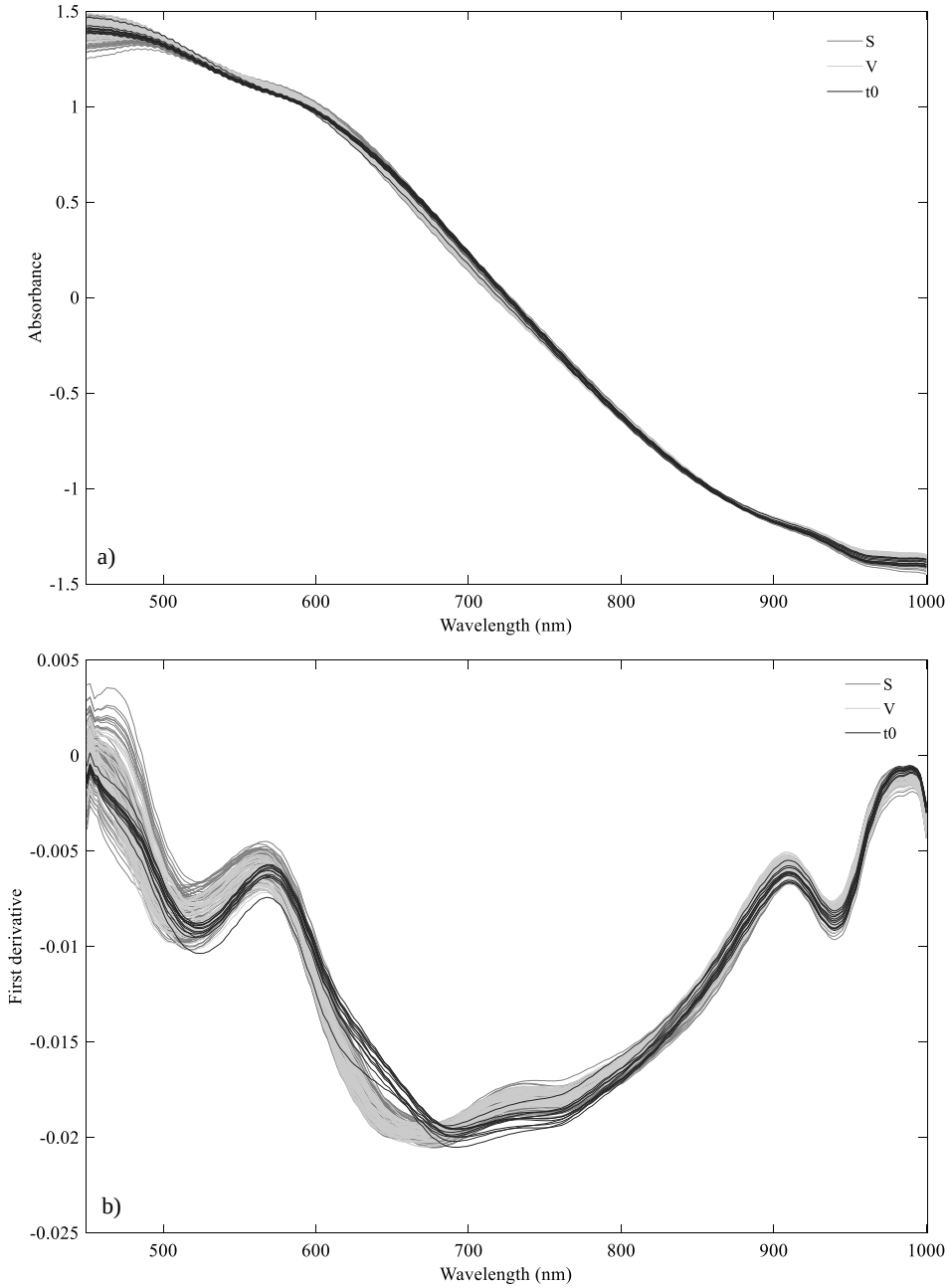

479

480 Fig.6

481

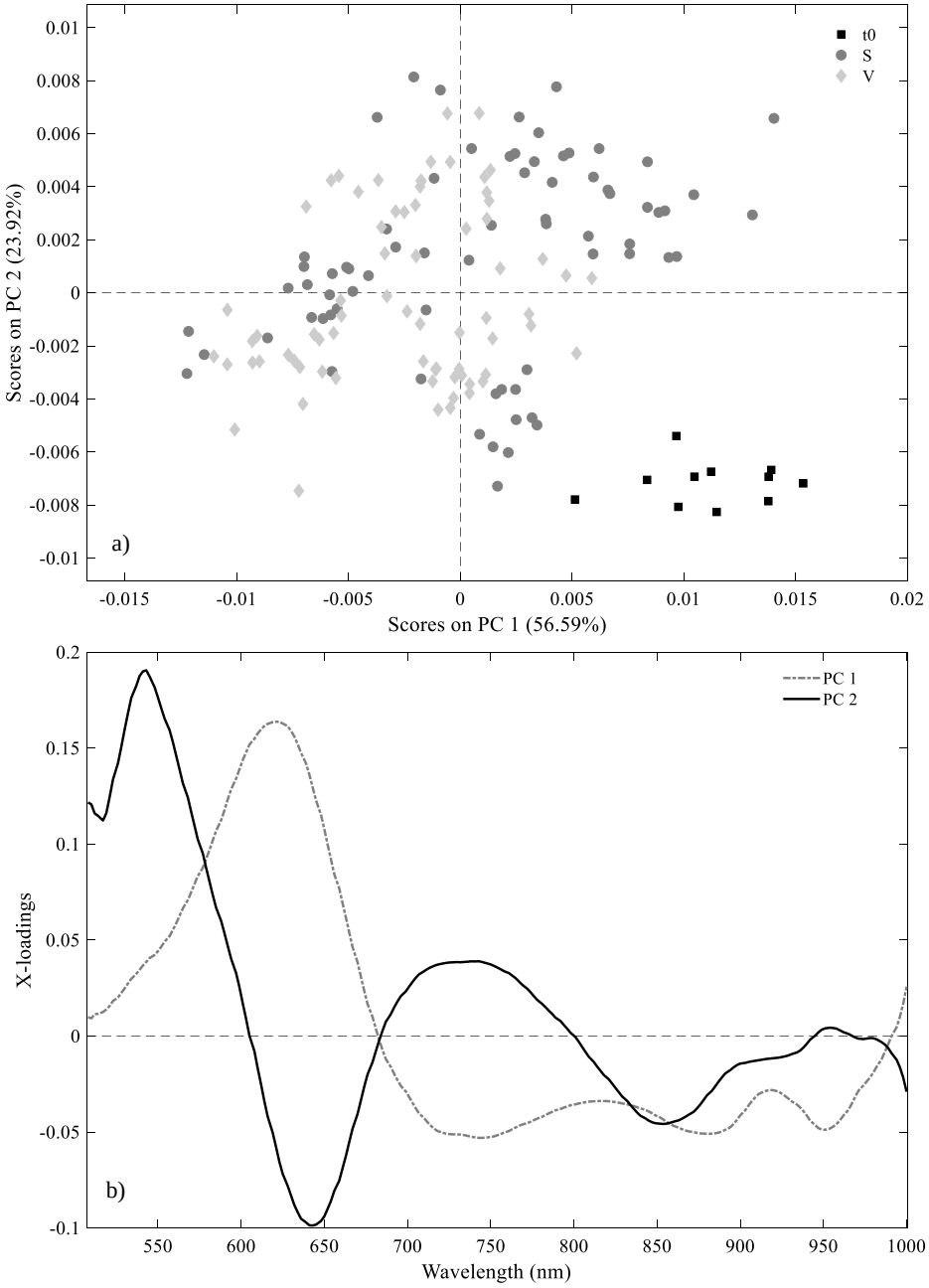

482

483 Fig.7

484

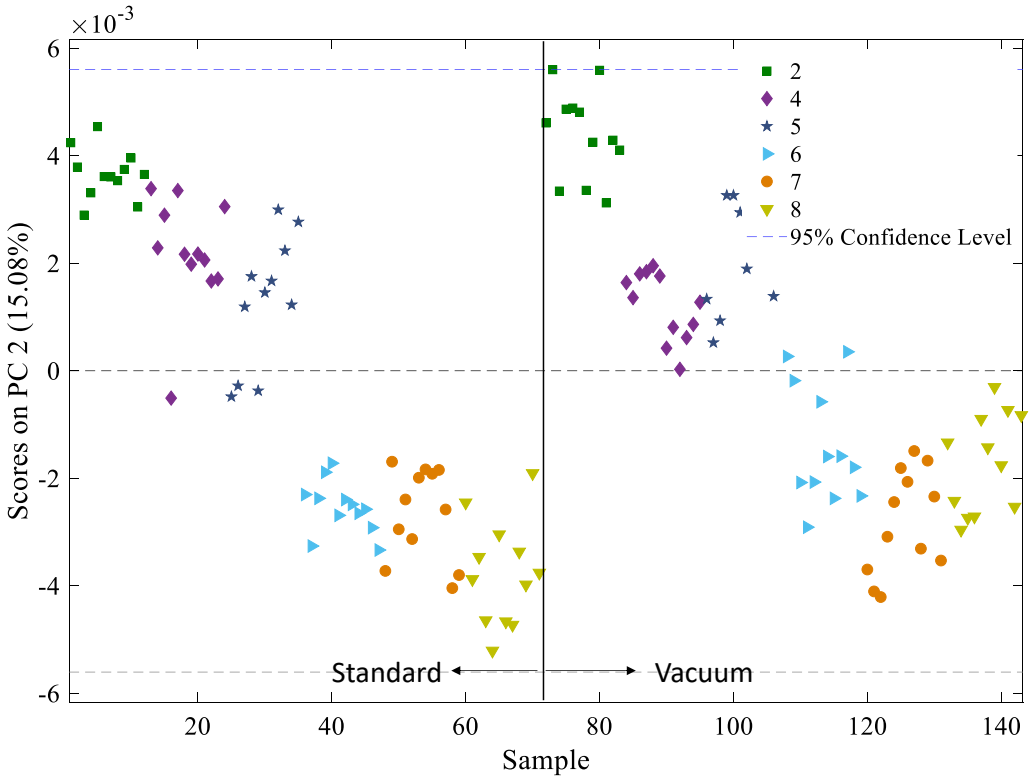

485

486 Fig.8

487

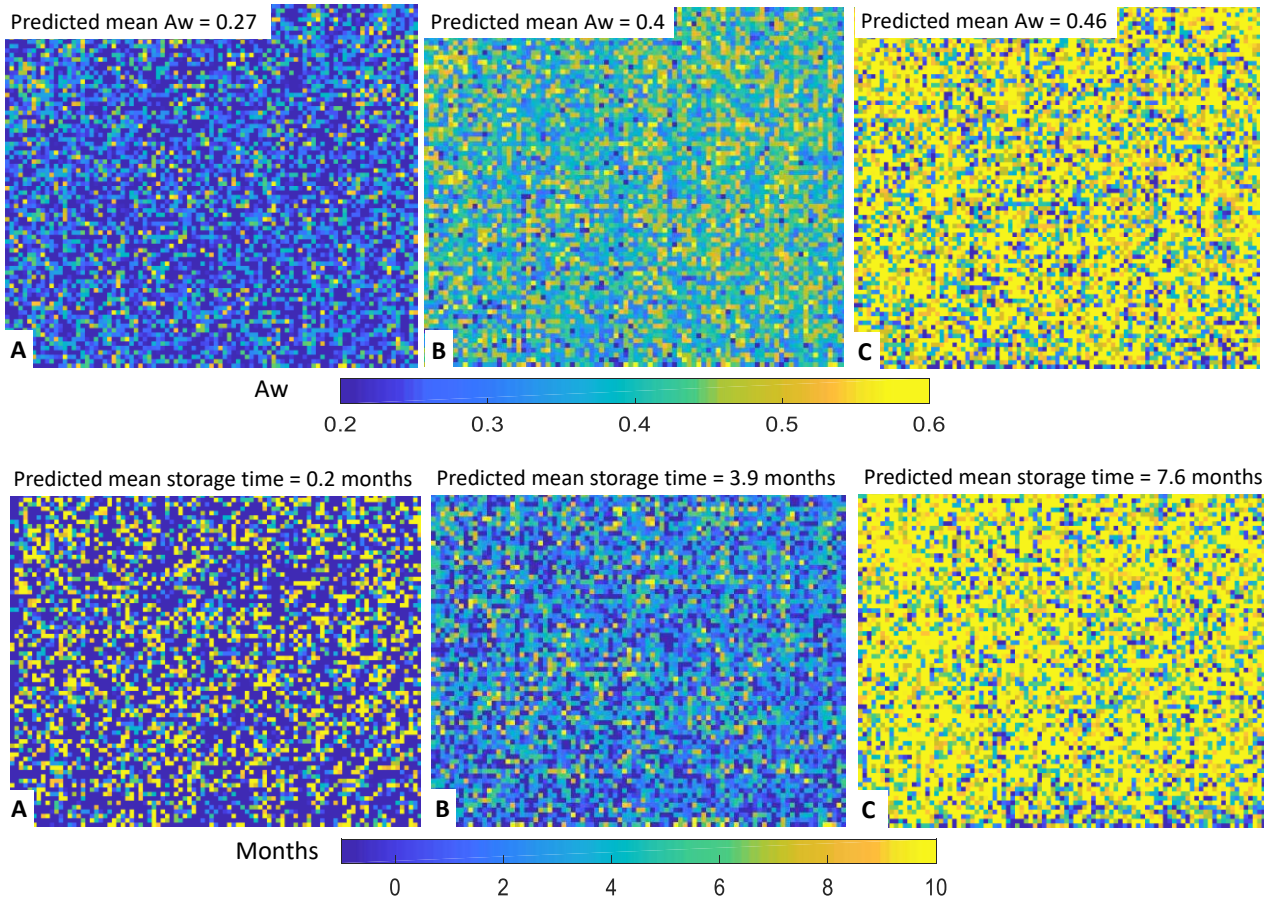

488

489 Fig.9

490

491 **Table 1:** Wafer cookie ingredients

 	
Wafer sheet (15.6%)	Wheat flour, potato starch, coconut oil, skimmed milk powder, sugar, soy whole flour, emulsifier: soy lecithin; egg yolk powder, raising agents: sodium carbonates, diphosphates; salt.
Vanilla cream (58.1%)	Coconut oil, sugar, dextrose, Skimmed milk powder, soy whole flour, salt, flavourings, Bourbon vanilla pod extract.
Chocolate enrobing (26.3%)	Cocoa paste, sugar, cocoa butter, emulsifier: soy lecithin; vanilla extract.

492

493

494 **Table 2**: Packaging materials

Packaging I	Packaging II	Packaging III
		
1) Multimaterial: wax paper (5 µm) and aluminum (10 µm 2) Paper	3) Calendered PVC film (300 µm) 4) Paper box (weight 400 gsm) 5) POF shrink film (19 µm)	6) Multimaterial: PET (12 µm), aluminium (8 µm) and PE (110 µm).

495

496

497

Table 3: Means and standard deviations (in brackets) of water activity (Aw), mechanical parameters (Fmax and D) and white index (WI) evaluated during the storage.

Packaging	Storage time (months)	Aw		F max (N)		D (N/mm)		WI	
S	0	0.27^{a}	(0.01)	50.63^{a}	(8.45)	1.09^{a}	(0.12)	32.06^{a}	(0.59)
	2	0.38^{b}	(0.01)	68.86^{b}	(7.89)	1.29^{b}	(0.13)	32.55^{a}	(0.45)
	4	0.39^{b}	(0.01)	68.19^{b}	(12.18)	1.35^{b}	(0.15)	32.45^{a}	(0.34)
	5	0.39^{b}	(0.01)	59.60^{a,b}	(8.71)	1.38^{b}	(0.12)	32.82^{a}	(0.44)
	6	0.41^{c}	(0.01)	65.15^{a,b}	(9.46)	1.30^{b}	(0.15)	32.18^{a}	(0.29)
	7	0.43^{d}	(0.01)	67.26^{b}	(9.27)	1.56^{c}	(0.15)	31.96^{a}	(0.53)
	8	0.47^{e}	(0.01)	57.16^{a}	(7.16)	1.55^{c}	(0.14)	32.38^{a}	(0.46)
V	0	0.27^{a}	(0.01)	50.63^{a}	(8.45)	1.09^{a}	(0.12)	32.06^{a}	(0.59)
	2	0.36^{b}	(0.01)	68.05^{b}	(6.23)	1.39^{b}	(0.11)	32.24^{a}	(0.46)
	4	0.38^{b}	(0.01)	59.12a^{a,b}	(10.29)	1.42^{b}	(0.15)	32.79^{a}	(0.35)
	5	0.38^{b}	(0.01)	61.74^{a,b}	(9.85)	1.30^{b}	(0.11)	32.65^{a}	(0.45)
	6	0.38^{b}	(0.01)	71.35^{b}	(9.40)	1.31^{b}	(0.12)	32.42^{a}	(0.32)
	7	0.40^{c}	(0.01)	69.33^{b}	(8.12)	1.56^{c}	(0.13)	32.63^{a}	(0.37)
	8	0.42^{d}	(0.01)	51.10^{a}	(7.39)	1.58^{c}	(0.12)	32.01^{a}	(0.45)

Note: S: standard packaging; V: vacuum packaging. Within the same type of packaging (S or V), means with the same letters are not significant different ($p<0.05$)

503 **Table 4:** Results of the PLS models developed to estimate the storage time and water activity from
504 NIR spectroscopy and Vis/NIR HIS data.

	Parameter	Samples	LV	Calibration		Cross-validation	
				R^2	RMSEC	R^2	RMSECV
NIR spectroscopy	Storage time (0-8 months)	S	10	0.989	0.26	0.958	0.53
		V	11	0.987	0.29	0.960	0.52
		S+V	12	0.956	0.49	0.926	0.63
	Water activity	S (0.27-0.47)	7	0.951	0.01	0.924	0.02
		V (0.27-0.42)	7	0.922	0.01	0.878	0.02
		S+V (0.27-0.47)	7	0.887	0.02	0.858	0.02
Vis/NIR HSI	Storage time (0-8 months)	S	10	0.957	0.54	0.955	0.56
		V	11	0.956	0.42	0.956	0.55
		S+V	12	0.931	0.57	0.931	0.62
	Water activity	S (0.27-0.47)	4	0.936	0.01	0.928	0.02
		V (0.27-0.42)	7	0.905	0.01	0.876	0.02
		S+V (0.27-0.47)	8	0.884	0.02	0.869	0.02

505 *Note: S: standard packaging; V: vacuum packaging; LV: latent variable; R^2: determination coefficient; RMSE: root*
506 *mean square error.*

507

508